Effect of sulphonic acids on electrodeposition of nickel and its structural and corrosion behaviour

R. Sekar* and S. Jayakrishnan

The influence of methane sulphonic acid, naphthalene sulphonic acid and phenol sulphonic acid on the electrodeposition of nickel from a citrate buffered nickel bath was investigated. Solution characteristics such as cathode efficiency and throwing power have been assessed, and corrosion resistance of the coatings was measured by electrochemical impedance spectroscopy method. The X-ray diffraction pattern obtained for electrodeposited nickel showed a polycrystalline fcc structure. A uniform and pinhole free surface was observed under SEM analysis.

Keywords: Additives, Citrate bath, Electrodeposition of nickel, Impedance spectroscopy, Polycrystalline, Crystal size

Introduction

Nickel plating is one of the most widely used processes for decorative, functional and electroforming applications,[1–3] including undercoats for gold plating. Watts bath is the most popular nickel electroplating bath, and it usually consists of nickel sulphate, nickel chloride and boric acid. Boric acid is an essential ingredient for maintaining the pH of the electrolyte and producing good quality ductile deposits.[4] The additives and operating parameters have a complex relationship in terms of their influence on the deposition mechanism. The mechanism of Ni^{2+} reduction from acid sulphate solutions has been extensively studied by Epelboin *et al.* using Watts baths.[5–7] It was suggested that there were two successive Faradaic reactions, the first involving the formation of Ni^{+}_{ads} followed by subsequent reduction to Ni. However, the adsorbed species of H^{*}_{abs} inhibited the hydrogen evolution in presence of freshly deposited nickel, which strongly bonds to the electrode surface and inhibits reduction. From an electrolyte of pH 2–4, the following deposition mechanisms have been suggested[8,9]

$$2(H^{+} + e^{-}) \rightarrow H_2 \quad (1)$$

$$Ni^{2+} + e^{-} \rightarrow Ni^{+}_{ads} \quad (2)$$

$$Ni^{+}_{ads} + e^{-} \rightarrow Ni \quad (3)$$

$$2H^{*}_{ads} \rightarrow H_2 \quad (4)$$

$$Ni^{+}_{ads} + H^{*}_{ads} + e^{-} \rightarrow Ni + H_{included} \quad (5)$$

Citric acid and citrate are used as buffering and complexing agents for autocatalytic nickel deposition[10] and electroplating of bright nickel,[11] iron alloy,[12] Ni–W alloy[13] and Cu–Ni alloy.[14] Citrate ions react with nickel ions to form nickel citrate complexes adsorbing on the cathode surface. Reports from Japan discuss the strict environmental protection regulations restricting dumping of waste streams containing boric acid.[15] As an eco-friendly alternative to boric acid in nickel plating baths, the authors have worked on developing a new bath using citrate instead of boric acid.

Organic additives are added in traces to electroplating baths to modify the surface morphology, structure, crystal size and physical properties such as hardness and wear resistance of the metal deposits.[16] For nickel plating from a Watts bath, commonly used brightener additives are aromatic sulphonones or sulphonates and compounds containing unsaturated groups such as >C=O, >N–C=S, –C=N, etc. Pewnim and Roy[17] have studied the codeposition of copper and tin using a methane sulphonic acid based electrolyte. Danilov *et al.*[18] have studied the kinetics of nickel ion electroreduction from a methanesulphonate electrolyte. In the present communication, results pertaining to characteristics of deposits from a bath containing nickel sulphate, nickel chloride and tripotassium citrate in the presence of sulphonic acids as additives are reported.

Experimental

The experiments were carried out in triplicate with copper specimens. Surface preparation before deposition is an important factor and can be achieved by mechanical and electrochemical methods.[19–21] The procedure adopted was removal of surface scales using mechanical polishing to get a smooth surface, degreasing with trichloroethylene and final electrocleaning at 4 A dm^{-2} in a solution of Na_2CO_3 (20 g L^{-1}), NaOH (7 g L^{-1}) and trisodium orthophosphate (9 g L^{-1}). Copper panels $7{\cdot}5 \times 5 \times 0{\cdot}1$ cm in size were used as cathodes in an electroplating assembly consisting of two 99·99% pure nickel anodes on either side of the cathode. The four nickel plating baths studied (A,

Electroplating and Metal Finishing Technology Division, Central Electrochemical Research Institute, Karaikudi, Tamil Nadu 630006, India

*Corresponding author, email grsek2004@yahoo.com

© 2012 Institute of Metal Finishing
Published by Maney on behalf of the Institute
Received 11 October 2011; accepted 07 March 2012
DOI 10.1179/0020296712Z.00000000032

B, C and D) are shown in Table 1, and they were operated at 50°C and at different current densities. The cathode current efficiency and plating rate in each case were calculated by weighing the cathode before and after deposition. Throwing power was measured using a Haring and Blum cell.[22–24] This is a rectangular cell consisting of two copper sheet cathodes $7{\cdot}5 \times 5 \times 0{\cdot}1$ cm in size filling the entire cross-section at opposite ends and one perforated nickel anode of the same size. The latter was placed between the cathodes so that its distance from one of the cathode was one-fifth its distance from the other. Values of throwing power (%) for different solutions used were calculated using Field's formula

$$\text{Throwing power} = \frac{L-M}{L+M-2} \times 100$$

where M is the metal distribution ratio between the near and far cathode, and L is the ratio of the respective distances of the far and near cathode from the anode.

To evaluate the adhesion of the nickel deposits on copper with various current densities, a bend test was employed. In this test, the specimen was bent back and forth at 180° until fracture of the basis metal occurs. Flaking or peeling of the deposit, if any, indicates poor adhesion.[25,26] Corrosion properties of nickel deposits were assessed based on electrochemical impedance spectra analysis. For these studies, nickel electrodeposited specimens were masked to expose 1 cm^2 of area on one side and used as the working electrode. A platinum foil ($2{\cdot}5 \times 2{\cdot}5$ cm) and a saturated calomel electrode were employed as counter electrode and reference electrode respectively; 3·5% sodium chloride was used as test solution. The impedance behaviour was studied in the test electrolyte for nickel deposits of 12 μm thickness. The working electrode was introduced into the test solution and allowed to attain a steady potential value.

The ac impedance measurements were carried out on nickel deposits in 3·5% sodium chloride solution at open circuit potential using an EG&G model 6310 frequency response analyser and applying an ac signal of 10 mV in the frequency range of 10 kHz to 1 MHz. The values of solution resistance R_s, double layer capacitance c_{dl} and charge transfer resistance R_{ct} were obtained from Nyquist plots of the real Z_{re} versus imaginary Z_{im} components, and corrosion resistance of the coating was determined from the R_{ct} value using the Stern–Geary equation[27]

$$I_{corr} = \frac{b_a\, b_c}{2{\cdot}303\,(b_a + b_c)} \times \frac{1}{R_{ct}}$$

where b_a and b_c are Tafel slopes.

X-ray diffraction patterns were obtained for nickel deposits from the four nickel plating baths (A, B, C and D) at 50°C. The samples were scanned at 30–80° (2θ) at a scan rate of 1° min^{-1} using Cu K_α ($\lambda = 1{\cdot}5405$ Å) radiation using the X'Pert PRO powder diffraction system PE 3040/60. The peaks due to the different planes were identified, and the corresponding lattice parameters were calculated. The crystal size of the nickel deposits was also measured using the Scherrer formula[28] from the predominant peak

$$t = \frac{0{\cdot}9\lambda}{\beta \cos \theta_B}$$

In order to understand the nature of the deposits obtained, the deposits obtained from different baths were studied visually and using scanning electron microscopy (SEM). Images of SEM were taken with JEOL JSM-35 LF at 25 kV with magnification of ×1000.

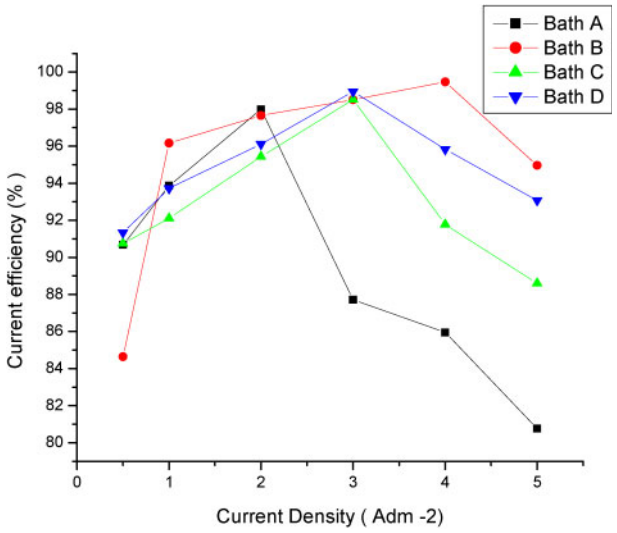

1 Effect of varying current density on current efficiency obtained from various baths at 50°C

Results and discussion

Cathode current efficiency and throwing power

The bath compositions are shown in Table 1. The results of the cathode current efficiency experiments were carried out at different current densities (0·5–5·0 A dm^{-2}) from the different nickel plating baths at 50°C, and the results are given in Fig. 1. For bath A, Fig. 1 shows that the cathode current efficiency gradually increases for current densities up to 2 A dm^{-2} and thereafter decreases with the increase in the current density. This may be due to hydrogen evolution at higher current densities. A smooth uniform deposit was observed between 0·5 and 3·0 A dm^{-2} and dull deposits between 4 and 5 A dm^{-2}. From these results, 0·5–2·0 A dm^{-2} was selected as being suitable for producing a smooth uniform deposit. The results of studies from bath B (Fig. 1) show the cathode current efficiency steadily increasing for current densities up to 4·0 A dm^{-2} and then slightly decreasing. Bright, mirror deposits were produced between 0·5 and 3·0 A dm^{-2}, and bright deposits with edge build-up were

Table 1 Bath composition of nickel baths studied

Bath	Constituents	Additives concentration
A	240 g L^{-1} nickel sulphate	Nil
B	40 g L^{-1} nickel chloride 20 g L^{-1} tripotassium citrate	1 mL L^{-1} methane sulphonic acid
C		1 g L^{-1} naphthalene sulphonic acid
D		1 g L^{-1} phenol sulphonic acid

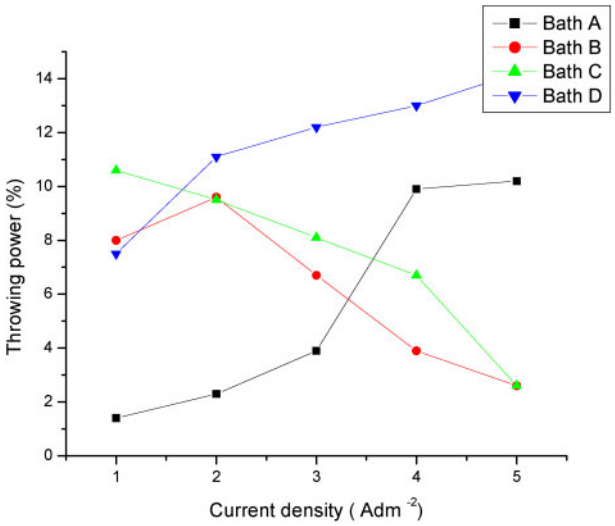

2 Effect of varying current density on throwing power for different baths at 30°C

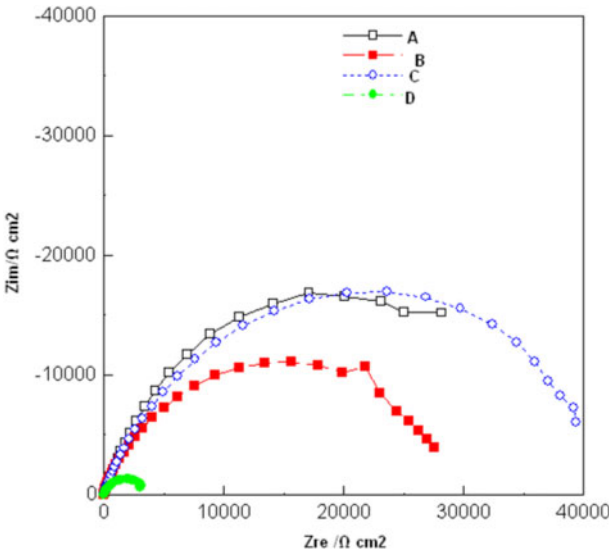

3 Typical EIS spectra obtained for various nickel deposits (12 μm) in 3·5% NaCl solution (A: bath A; B: bath B; C: bath C; D: bath D)

obtained between 4 and 5 A dm^{-2}. It may be concluded that 0·5–3·0 A dm^{-2} is more beneficial for producing a bright and mirror bright deposit. The results of studies from bath C (Fig. 1) indicate that the cathode current efficiency steadily increases at current densities from 0·5 to 3·0 A dm^{-2} and thereafter gradually decreases, probably through hydrogen evolution at high current densities. Bright and mirror bright deposits are produced between 0·5 and 3·0 A dm^{-2}. Bath D (Fig. 1) produced a bright deposit between 0·5 and 3·0 A dm^{-2}, and pitted deposits were observed >4 A dm^{-2}.

Figure 2 gives the variation of throwing power of baths A, B, C and D with different current densities. Throwing power of bath A (Fig. 2) increased with current density, which may be attributed to the increase in cathodic polarisation with increasing current density.

With the addition of methane sulphonic acid at 1 mL L^{-1} as additive in bath B (Fig. 2), the throwing power increases up to 2 A dm^{-2} and thereafter gradually decreases. This may be due to hydrogen evolution at high current densities. With the introduction of naphthalene-2-sulphonic acid as an additive in bath C (Fig. 2), high throwing power was observed at low current density, which steadily decreases with increasing current densities. This may be due to adsorption of the additive on the electrode surface. With the addition of phenol sulphonic acid at 1 g L^{-1} in bath D (Fig. 2), throwing power increases with current density, and it can be observed that the throwing power is highest in this bath as compared to the other three.

Adhesion

Adhesion of the nickel deposits obtained in the presence and absence of additives from the nickel bath was tested by subjecting the plated specimens to standard bend tests. The deposits from all four baths were found to withstand the bend test, showing that the keying and adhesion of the deposit to the base metal were very good in all cases.

Electrochemical impedance spectroscopy (EIS) measurements

The technique of EIS is one of the most intensively used non-destructive and powerful techniques for the investigation and prediction of corrosion protection. The EIS represents the way in which charges are transferred or impeded between various phases, which may be studied by the status and behaviour of interfaces among conducting phases.[29] It is well known that if the process is purely charge transfer controlled, the impedance spectrum will be a perfect semicircle.[30] The shape of the impedance spectra supports the assumption that the polarisation resistance R_p value is the same as the charge transfer resistance R_{ct}, which is easily estimated on the real impedance axis by extrapolating the impedance trend at the lowest frequencies. The Nyquist plot obtained in 3·5% sodium chloride solution is shown in Fig. 3. Curve A in Fig. 3 shows the impedance diagram obtained for the nickel deposit without any additive, whereas curves B, C and D show the EIS for Ni deposits produced from baths B, C and D with additives. The shapes of the impedance curves were semicircular, indicating charge transfer control of corrosion of nickel deposits obtained from all four baths. As the diameter of the capacitive semicircle represents the resistance of the coating, it can be said that the protective properties of the coatings increase with increasing diameter of the semicircle.[31,32] Among the four deposits studied, the deposit produced from the bath containing naphthalene-2-sulphonic acid (bath C) produced a large semicircle with high R_{ct} value of >40 000 Ω cm^2 on the real axis indicating the highest corrosion resistance. In general, the conditions that were favourable for good nickel deposition were characterised by a single loop at high frequency with low capacitance and high charge transfer resistance.[33]

X-ray diffraction analysis

Figure 4 shows X-ray diffraction patterns of the nickel electrodeposits obtained at 2 A dm^{-2} and at 50°C from baths A, B, C and D. All the deposits are crystalline in nature and have face centred cubic structure. The observed value (Table 2) is in good agreement with the standard value for nickel deposit. Figure 4*a* shows that the electrodeposited nickel coatings have a texture with (111), (200) and (220) planes observed, but the (111) plane

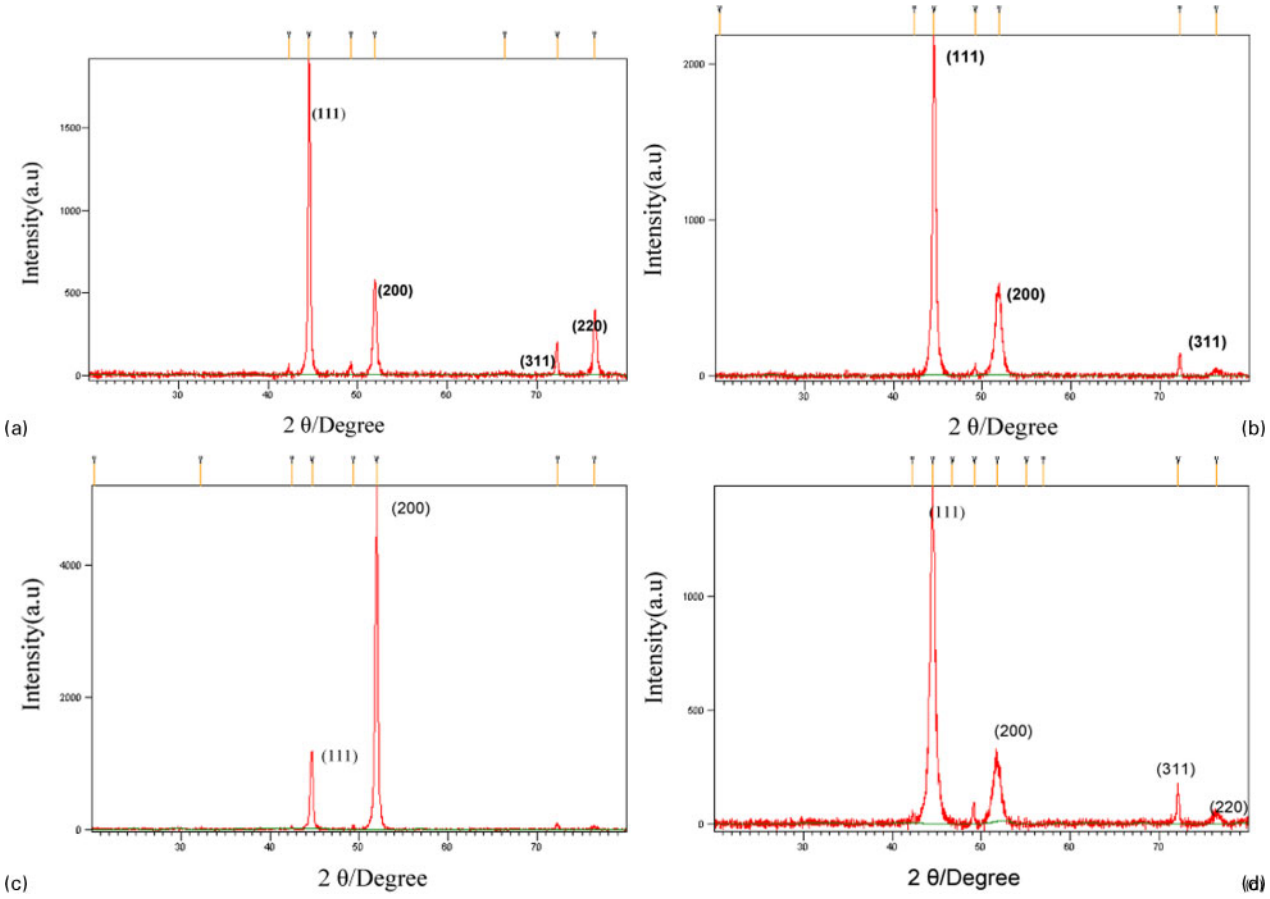

a bath A; *b* bath B; *c* bath C; *d* bath D

4 X-ray diffraction pattern for nickel deposits obtained at 2 A dm^{-2} and at 50°C

was more predominant and the other peak intensities were lesser. Similar observations have been made earlier by others.[34–37] Generally, current density increases are associated with decrease in grain size and modification of the texture.

Figure 4*b* indicates that for the deposit obtained from bath B, the (111) plane was more predominant and other peak intensities were reduced. This suggests that orientation changes occurred with the addition of methane sulphonic acid as additive in the electrolyte.

Figure 4*c* represents the X-ray diffraction pattern of the deposit produced from bath C. The (200) plane was more predominant, and the reflection of other peaks was reduced; the intensity of the (200) peak is highly increased. Hence, the deposit obtained from the naphthalene-2-sulphonic acid containing the bath showed that the crystallite growth in the direction of (111) and (311) was inhibited. These significant changes in the crystallographic orientations are reflected in the observed deposit morphology, which was smooth and compact.[38]

For the deposit obtained from bath D (Fig. 4*d*), the X-ray diffraction pattern shows a polycrystalline structure. The same (111) plane reflection was more predominant as in the case of baths A and B. Hence, the methane and phenol groups dominate the side reaction of hydrogen evolution, decrease the surface energy of the (111) crystallographic planes preferentially and encourage planar growth in the nickel. Thus, it is possible that the modification of the growth interface by hydrogen facilitates the formation of larger grains.[39] The crystal

Table 2 X-ray diffraction data for electrodeposited nickel obtained at 2 A dm^{-2} and at 50°C

Bath	'*d*' observed	'*d*' standard	*hkl*
A	2·0316	2·034	(111)
	1·7597	1·762	(200)
	1·307	1·259	(311)
	1·2452	1·246	(220)
B	2·0311	2·034	(111)
	1·7583	1·762	(200)
	1·307	1·259	(311)
C	2·0253	2·034	(111)
	1·7562	1·762	(200)
D	2·0388	2·034	(111)
	1·7643	1·762	(200)
	1·3089	1·259	(311)
	1·2462	1·246	(220)

Table 3 Crystal size for nickel deposits obtained from various baths at 2 A dm^{-2} and at 50°C

Bath	2θ value	Full width at half maximum 2θ value	Plane	Relative Intensity/%	Crystal size/nm
A	44·5626	0·2652	(111)	100	32·7
B	52·0308	0·2244	(111)	100	39·8
C	44·5742	0·3672	(200)	100	23·4
D	44·3968	0·2040	(111)	100	42·8

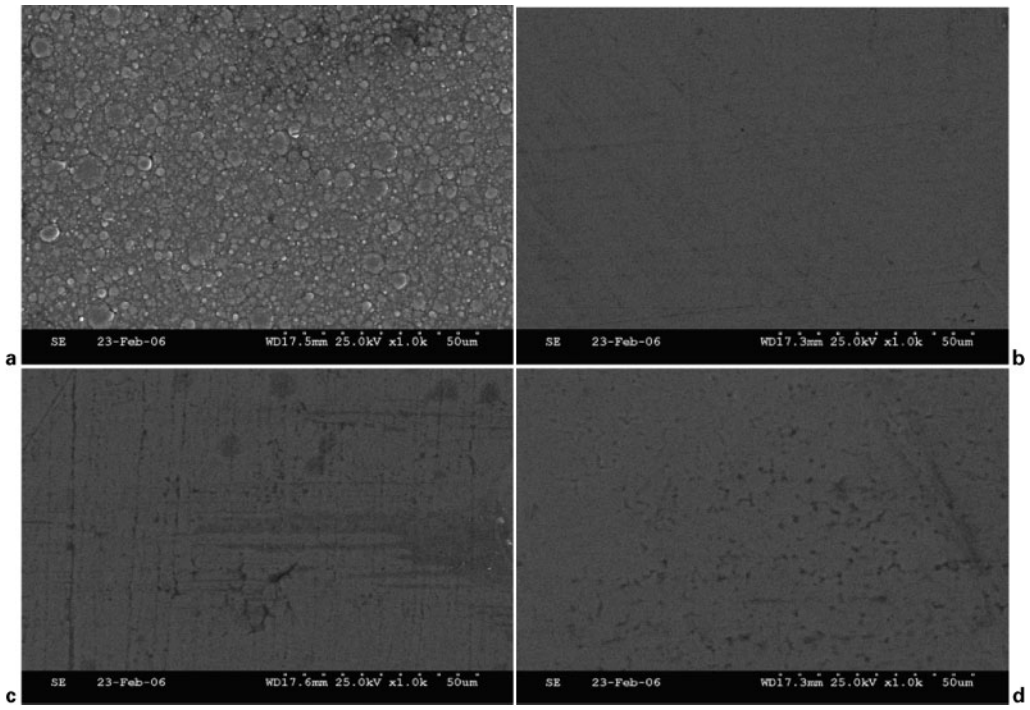

a bath A, additive free; *b* bath B, containing methane sulphonic acid (1·0 mL L^{-1}); *c* bath C, containing naphthalene sulphonic acid (1·0 g L^{-1}); *d* bath D, containing phenol sulphonic acid (1·0 g L^{-1})

5 Images (SEM) of nickel deposit obtained at 2 A dm^{-2} and at 50°C

size was measured in the predominant peak of the deposits produced from all baths.

Among these, the deposit obtained from the naphthalene sulphonic acid containing bath C showed that the crystal size is very small as compared to the other three baths (Table 3). Hence, naphthalene sulphonic acid appears to act as the best grain refiner. This was further confirmed by SEM analysis.

Microstructural characterisation

Figure 5 shows the surface morphology of the nickel deposits obtained from the four baths. In Fig. 5*a*, the surface morphology of the nickel deposit obtained from the bath without additive may be related to the texture for the deposits having relatively fewer imperfections in the crystal structure. The main feature is that the clusters of small spherical shaped nickel crystals are randomly arranged; they are face centred cubic in nature, and the large grain size is usually associated with low cathode polarisation. With the introduction of the methane sulphonic acid as additive into the plating bath, the surface morphology was changed from a spherical shaped structure into a fine grained structure. Hence, the morphology and the grain size are both dependent on the presence of additives. Figure 5*b–d* also indicates clearly that the use of the additives refined the grain size.

Conclusions

It was concluded that a smooth, uniform, dense and satin white deposit is obtained in the absence of additive using tripotassium citrate as a buffer for nickel electrodeposition. It offers good buffering capacity and is a more environmentally friendly substitute for boric acid in a Watts bath. In the presence of sulphonic acids such as methane sulphonic acid, naphthalene sulphonic acid and phenol sulphonic acid as additives, bright and adherent deposits of nickel can be electrodeposited. These baths produce deposits with high cathode efficiency and reasonable throwing power. The corrosion characteristics of the nickel deposits were evaluated by the EIS method. These studies reveal that the deposits obtained from a bath containing naphthalene sulphonic acid exhibited the highest R_{ct} value and have higher corrosion resistance. Hence, deposits obtained from bath C containing naphthalene sulphonic acid are compact, dense, non-porous and fine grained. X-ray diffraction studies revealed that the deposits obtained from baths A, B and D show predominance of (111) plane, in contrast to the deposit from bath C, which shows predominance of (200) plane. The crystal structures of the deposits obtained from the citrate based bath are dependent on the effect of operating parameters such as bath composition, current density, pH, temperature and type of additive used. Scanning electron microscopy studies showed that the deposits obtained in the absence of additives are small spherical shaped crystals that are randomly arranged, whereas the deposits obtained from baths containing additives are fine grained and of pore free morphology.

References

1. F. A. Lowenheim: 'Modern electroplating', 3rd edn; 1974, New York, John Wiley and Sons, Inc.
2. Metal Finishing guide book and directory, 1999: 276 Hackensack, NJ, Metals and plastics Publications Inc.
3. J. K. Dennis and T. E. Such: 'Nickel and chromium plating', 97; 1993, Cambridge, Woodhead Publishing Ltd.
4. D. Golodniky, N. V. Gudin and G. A. Volyanuk: *J. Electrochem. Soc.*, 2000, **147**, 4156–4163.
5. R. Wiart: *Electrochim. Acta*, 1990, **35**, 1587–1592.
6. F. Chassaing, M. Joussellin and R. Wirat: *J. Electroanal. Chem.*, 1983, **157**, 75–81.
7. I. Epelboin, M. Joussellin and R. Wirat: *J. Electroanal. Chem.*, 1981, **119**, 61–65.
8. S. Watson and R. Walters: *J. Electrochem. Soc.*, 1991, **138**, 3633–3637.
9. S. Watson: *J. Electrochem. Soc.*, 1993, **140**, 2235–2239.

10. R. Tarozaite, O. Glyliene and G. Stalnionis: *Surf. Coat. Technol*., 2005, **200**, 2208–2213.
11. T. Doi, K. Mizumoto, S. I. Tanakaand and T. Yamashita: *Met. Finish*., 2004, **102**, 26–35.
12. M. Ghorbani, A. G. Dolati and A. Afshar: *Russ. J. Electrochem*., 2004, **8**, 1173–1177.
13. O. Younes and E. Gileadi: *J. Electrochem. Soc*., 2002, **149**, C100–C111.
14. R. Y. Ying: *J. Electrochem. Soc*., 1988, **135**, 2957–2964.
15. T. Doi, K. Mizumoto, M. Kayashima and S. Tanaka *J. Surf. Finish. Soc. Jpn*, 2000, **51**, 718–722.
16. D. Pletcher: 'Industrial electrochemistry', 184; 1984, New York, Chapman and Hall.
17. N. Pewnim and S. Roy: *Trans. Inst. Met. Finish*, 2011, **89**, 206–209.
18. F. I. Danilov, I. V. Sknar and Y. E. Sknar: *Russ. J. Electrochem*, 2011, **47**, 1035–1042.
19. R. Sekar and S. Jayakrishnan: *Plat. Surf. Finish*., 2005, **92**, 58–68.
20. R. Sekar and S. Jayakrishnan: *J. Appl. Electrochem*., 2005, **36**, 591–597.
21. R. Sekar, C. Eagammai and S. Jayakrishnan: *J. Appl. Electrochem*., 2010, **40**, 49–57.
22. S. Shawki, F. Hanna and Z. A Hamid: *Met. Finish*., 1987, **85**, 59–56.
23. B. E. Conway and J. O'M. Bockris: *Plating*, 1959, **46**, 371–383.
24. R. Sekar, C. Kala and R. M. Krishnan: *Trans. Inst. Met. Finish*., 2002, **80**,173–176.
25. 'Adhesion of metallic coatings', ASTM test method B571-84:1995, 02.05, ASTM International, West Conshohocken, PA, USA, 1995.
26. N. Kanani: 'Electroplating – basic principles, processes and practice', 1st edn, 75; 2004, Berlin, Elsevier.
27. M. Stern and A. L. Geary: *J. Electrochem. Soc*., 1957, **104**, 56–63.
28. B. D. Cullity: 'Elements of X-ray diffraction'; 1967, Reading, MA, Addison-Wesley.
29. C. N. Cao and J. Q Zhang: 'An introduction to electrochemical impedance spectroscopy', 1st edn; 2002, Beijing, Science Press.
30. F. Mansfield, W. Kendig and S. Tsai: *Corrosion*, 1987, **38**, 570–580.
31. S. Survilline, A. Cesuniene and R. Juskena: *Trans. Inst. Met. Finish*., 2004, **82**, 185–189.
32. S. Survilline, A. Lisowska-oleksiak, V. Jasualaitiene and A. Cesuniene: *Trans. Inst. Met. Finish.*, 2005, **83**, 130–135.
33. M. Holm and T. J. O'Keefe: *J. Appl. Electrochem*., 2000, **30**, 1125–1132.
34. I. Fomov and M. Monev: *J. Appl. Electrochem*., 1992, **22**, 262–267.
35. Y. Wu, Y. Xiang, W. Hu, C. Zhao and W. Ding: *Trans. Inst. Met. Finish*. 2005, **2**, 91–94.
36. N. V. Pangarov: *Electrochim. Acta*, 1962, **7**, 139–146.
37. N. V. Pangarov: *Electrochim. Acta*, 1964, **9**, 721–726.
38. U. S. Mohanty, B. C. Tripathy, P. Singh and S. C. Das: *J. Appl. Electrochem*., 2001, **31**, 579–583.
39. K. Hang and T. Jenkins: *J. Phys. Chem. B*, 2000, **104B**, 10017–10021.